THE JOURNAL OF BIOLOGICAL CHEMISTRY VOL. 286, NO. 40, pp. 34593–34605, October 7, 2011

Diabetes and Pancreatic Exocrine Dysfunction Due to Mutations in the Carboxyl Ester Lipase Gene-Maturity Onset Diabetes of the Young (*CEL*-MODY)

A PROTEIN MISFOLDING DISEASE[*][S]

Received for publication, January 19, 2011, and in revised form, July 15, 2011 Published, JBC Papers in Press, July 22, 2011, DOI 10.1074/jbc.M111.222679

Bente B. Johansson,[a,b] Janniche Torsvik,[a,b] Lise Bjørkhaug,[a,b] Mette Vesterhus,[a,c] Anja Ragvin,[a,b] Erling Tjora,[a,c] Karianne Fjeld,[a,b] Dag Hoem,[d,e] Stefan Johansson,[a,b] Helge Ræder,[a,c] Susanne Lindquist,[f] Olle Hernell,[f] Miriam Cnop,[g,h] Jaakko Saraste,[i] Torgeir Flatmark,[i] Anders Molven,[e,j] and Pål R. Njølstad[a,c1]

From the [a]Department of Clinical Medicine, University of Bergen, N-5020 Bergen, Norway, the [b]Center for Medical Genetics and Molecular Medicine, Haukeland University Hospital, N-5021 Bergen, Norway, the Departments of [c]Pediatrics and [d]Surgery, Haukeland University Hospital , N-5021 Bergen, Norway, the [e]Section for Pathology, the Gade Institute, University of Bergen, N-5021 Bergen, Norway, the [f]Department of Clinical Sciences, Pediatrics, Umeå University, SE-901 87 Umeå, Sweden, the [g]Laboratory of Experimental Medicine, Université Libre de Bruxelles, B-1070 Brussels, Belgium, [h]Division of Endocrinology, Erasmus Hospital, B-1070 Brussels, Belgium, the [i]Department of Biomedicine, University of Bergen, N-5020 Bergen, Norway, and the [j]Department of Pathology, Haukeland University Hospital, N-5021 Bergen, Norway

***CEL*-maturity onset diabetes of the young (MODY), diabetes with pancreatic lipomatosis and exocrine dysfunction, is due to dominant frameshift mutations in the acinar cell carboxyl ester lipase gene (*CEL*). As *Cel* knock-out mice do not express the phenotype and the mutant protein has an altered and intrinsically disordered tandem repeat domain, we hypothesized that the disease mechanism might involve a negative effect of the mutant protein. *In silico* analysis showed that the p*I* of the tandem repeat was markedly increased from pH 3.3 in wild-type (WT) to 11.8 in mutant (MUT) human CEL. By stably overexpressing CEL-WT and CEL-MUT in HEK293 cells, we found similar glycosylation, ubiquitination, constitutive secretion, and quality control of the two proteins. The CEL-MUT protein demonstrated, however, a high propensity to form aggregates found intracellularly and extracellularly. Different physicochemical properties of the intrinsically disordered tandem repeat domains of WT and MUT proteins may contribute to different short and long range interactions with the globular core domain and other macromolecules, including cell membranes. Thus, we propose that *CEL*-MODY is a protein misfolding disease caused by a negative gain-of-function effect of the mutant proteins in pancreatic tissues.**

Most monogenic forms of diabetes are due to mutations in genes expressed in the pancreatic beta cell. Previously, Raeder *et al.* (1) reported a novel monogenic syndrome caused by mutations in the carboxyl ester lipase gene (*CEL*) (OMIM 609812; *CEL*-MODY[2] or MODY8), characterized by dominantly inherited childhood-onset pancreatic exocrine dysfunction and diabetes mellitus from adulthood. Notably, this gene is not transcribed in beta cells but is mainly expressed in pancreatic acinar tissue (2, 3) and lactating mammary glands (4, 5). The CEL enzyme (EC 3.1.1.13), also known as bile salt-stimulated/dependent lipase, is secreted into the intestine and activated by bile salts, playing a role in the hydrolysis and absorption of cholesterol- and lipid-soluble vitamins (6).

The human *CEL* gene is ~10 kb in size and consists of 11 exons. In the last exon, there is a variable number of tandem repeats (VNTR) where the 33-bp nearly identical segments are repeated usually between 7 and 23 times (1, 7–9). The VNTR of the most common *CEL* allele has 16 repeats, thereby encoding a protein consisting of 745 amino acids with a predicted molecular mass of ~79 kDa. The rat Cel is secreted from the acinar cells and is thought to follow the classical pathway of secretory proteins (for review see Ref. 3). In the endoplasmic reticulum (ER), the protein is co-translationally *N*-glycosylated at a conserved Asn residue (Asn-210), serving as a client protein for the molecular chaperone GRP94 and being associated with ER membranes (10, 11). The VNTR-encoded protein C terminus is heavily *O*-glycosylated in the mature protein, probably on Thr residues before or after PVPP motifs in the first 10 repeats (12). The *O*-glycosylation sites are present in a region enriched in the amino acids proline, glutamate, serine, and threonine (PEST sequence), a signal for rapid protein degradation, and glycosylated CEL is hypothesized to escape PEST-mediated degradation (10, 13, 14). Once fully glycosylated at the *trans*-Golgi network, the enzyme is phosphorylated by casein kinase II on

* The work was supported by a grant from the Translational Fund of the Bergen Medical Research Foundation (to A. M. and P. R. N.), the University of Bergen, Haukeland University Hospital, Helse Vest, Innovest, the FUGE Program at the Research Council of Norway (to P. R. N.), and Fonds National de la Recherche Scientifique-Fonds de la Recherche Scientifique Médicale (to M. C.).

[S] The on-line version of this article (available at http://www.jbc.org) contains supplemental Methods, Figs. S1–S5, and additional references.

[1] To whom correspondence should be addressed: Section for Pediatrics, University of Bergen, Haukeland University Hospital, N-5021 Bergen, Norway. Tel.: 47-55975153; Fax: 47-975159; E-mail: pal.njolstad@uib.no.

[2] The abbreviations used are: MODY, maturity onset diabetes of the young; CEL, carboxyl ester lipase; IAPP, islet amyloid polypeptide; RRL, rabbit reticulocyte lysate; TR, tandem repeat; UPR, unfolded protein response; VNTR, variable number of tandem repeats; MUT, mutant; ER, endoplasmic reticulum; EV, empty vector; BisTris, 2-[bis(2-hydroxyethyl)amino]-2-(hydroxymethyl)propane-1,3-diol.

Thr-363 (15, 16), which promotes its release from membranes, translocation through the secretory pathway, and co-storage with other digestive enzymes in secretory granules. CEL represents 4–8% of the total secreted protein in human pancreatic juice (17).

Although pancreatic lipomatosis and exocrine dysfunction are early events in the development of *CEL*-MODY dysfunction (1, 18), the pathogenic mechanism involved is unknown. In a recent study, our group found that knocking out *Cel* in mice did not result in diabetes or exocrine dysfunction, indicating that *CEL*-MODY is not due to haploinsufficiency (19). Because the mutant proteins in the two described families of Raeder *et al.* (1) were found to be very similar in sequence and both are predicted to be altered compared with the normal protein, we anticipated that the mechanism of disease may involve a negative gain-of-function effect of the mutant proteins, which would be detectable in cellular model systems. We therefore stably overexpressed the human CEL wild-type (CEL-WT) and mutant (CEL-MUT) proteins in human embryonic kidney (HEK293) cells and investigated the biosynthesis, glycosylation, secretion, and intracellular fate of the two protein variants.

EXPERIMENTAL PROCEDURES

Stable Expression of CEL-WT and CEL-MUT in HEK293 Cells—We cultured HEK293 cells (Clontech) in α-minimal essential medium (Sigma) supplemented with 4 mM L-glutamine (Sigma), 10% (v/v) fetal bovine serum (Invitrogen), and 100 units/ml penicillin/streptomycin (Invitrogen). Subconfluent (70–80%) cells were transiently transfected with pcDNA3.1/V5-His plasmids (see supplemental Methods and supplemental Fig. S1) containing CEL-WT, CEL-MUT, or the empty vector (EV) by FuGENE 6 transfection reagent (Roche Diagnostics) according to the manufacturer's instructions; a ratio of 3 μl of transfection reagent per μg of DNA was used. For stable CEL expression, we selected the cells with 500 μg/ml geneticin 418 (G418) (Invitrogen) in the culture medium for 18 days, followed by isolation of G418-resistant colonies. Cells with suitable CEL expression were clonally expanded, and clones with similar expression and transcription levels (supplemental Fig. S2) were chosen for further studies. We maintained the selected stable cell lines in culture medium containing 500 μg/ml G418.

Metabolic Labeling—3.5×10^5 HEK293 cells were seeded on polylysine-coated 35-mm dishes and grown in α-modified Eagle's medium, supplemented with 10% (v/v) fetal bovine serum for 24 h. We performed metabolic labeling by rinsing the cells stably expressing CEL-WT and CEL-MUT with phosphate-buffered saline (PBS) followed by incubation for 1 h in Met/Cys-free DMEM (Sigma) in the absence of serum, and with further incubation for 5 min in this medium supplemented with 110 μCi/ml [^{35}S]Met/Cys (PerkinElmer Life Sciences). The monolayers were washed with PBS and chased in DMEM containing an excess of cold Met and Cys. To determine the effects of proteasomal (MG132, Biomol, Plymouth Meeting, PA) and lysosomal (leupeptin, Sigma) protease inhibitors, cells were treated with the inhibitors for 3 h before the chase, and the inhibitors were also present throughout the chase at the following concentrations: 10 μM MG132 (dissolved in DMSO; vehicle control at an equal concentration of DMSO) and 100 μg/ml leupeptin. The cells were lysed in RIPA buffer, and the CEL protein was isolated by immunoprecipitation and analyzed by SDS-PAGE (see supplemental Methods).

Protein Deglycosylation—Cell growth medium from stably transfected HEK293 cells (50 μl) was acetone-precipitated (medium/acetone, 1:4) at −20 °C for 1 h, and the proteins were recovered by centrifugation at 13,000 rpm for 30 min at 4 °C. The acetone was evaporated, and the pelleted proteins were resuspended in SDS denaturation buffer (20 mM phosphate buffer, pH 7.5, 1% (w/v) SDS, 1% (v/v) β-mercaptoethanol) and incubated at 100 °C for 10 min. We treated the proteins with glycosidases at 37 °C for 18 h in 150 μl of a medium containing 100 mM phosphate buffer, pH 7.5, 20 mM EDTA, 0.5% (v/v) Nonidet P-40, 1% (v/v) β-mercaptoethanol, 2 units of *N*-glycosidase F (Roche Diagnostics) or 2.5 milliunits of *O*-glycosidase (Roche Diagnostics) or 5 milliunits of neuraminidase (Roche Diagnostics). After incubation, samples were subjected to SDS-PAGE and immunoblot analysis (supplemental Methods) using the mouse anti-V5 antibody (Invitrogen).

Native-PAGE—Three 35-mm dishes of stably transfected HEK293 cells were metabolically labeled for 5 min and chased for 45 min. We lysed the cells in 333 μl/dish of FastBreak lysis buffer (Promega, San Luis Obispo, CA) and purified the CEL proteins using the MagneHis Protein purification system (V8500; Promega) according to the manufacturer's instructions. The CEL proteins were eluted in 50 μl of 500 mM imidazole, 100 mM Hepes buffer, pH 7.5, and native-PAGE sample buffer was added as recommended by Promega. After centrifugation at 435,000 × *g* for 1 h at 4 °C, the supernatants were analyzed by native-PAGE (Novex 3–12% BisTris gel, Invitrogen) run at 150 V for 1.5 h. The gels were fixed, dried, and the labeled bands detected by a phosphorimager. The 435,000 × *g* pellets were resuspended in a SDS-containing buffer and heated at 56 °C for 15 min prior to NuPAGE 4–12% BisTris gels (Invitrogen) at 150 V for 2 h. The gels were immunoblotted using rabbit anti-V5 (1:15,000) (V8137, Sigma) and goat anti-rabbit-HRP secondary antibody (1:20,000) (sc-2313, Santa Cruz Biotechnology) at room temperature (RT). The CEL proteins were detected and the signals quantified using enhanced chemiluminescence on an imager.

Subcellular Fractionation and Determination of Triton X-100-soluble and -insoluble CEL-MUT Protein—The HEK293 cells were cultured in 75-cm^2 flasks until 80–90% confluent, washed, and harvested in Hanks' balanced salt solution (Invitrogen) and pelleted by centrifugation (300 × *g* for 5 min 4 °C). We resuspended the pellets in ice-cold homogenization medium (130 mM KCl, 25 mM NaCl, 1 mM EGTA, 25 mM Tris-HCl, pH 7.4) supplemented with protease inhibitor mixture (Complete Mini, Roche Diagnostics). Resuspended cells were homogenized by 20 passages through a ball-bearing cell cracker (EMBL, Heidelberg, Germany) with a clearance of 0.01 mm, and the extent of breakage was checked by phase contrast microscopy (20). The nuclei and cell debris were removed by centrifugation at 600 × *g* for 10 min at 4 °C, and the post-nuclear supernatant was recentrifuged at 3,000 × *g* for 10 min at 4 °C. Samples (0.6 ml) of the 3,000 × *g* supernatant and the pellet (resuspended in 0.6 ml homogenization medium) were

treated with 1% (v/v) Triton X-100 (Sigma) for 30 min and centrifuged at 100,000 × *g* for 1 h at 4 °C; the supernatants were referred to a Triton X-100-soluble CEL protein. The resulting pellets were finally solubilized by sonication in 5 M guanidine chloride buffered at pH 8 with 50 mM Tris, containing protease inhibitor mixture, incubated overnight at room temperature, and centrifuged at 13,000 × *g* for 20 min. The supernatants, referred to as the Triton X-100-insoluble (guanidine chloride-soluble) CEL protein, were diluted 10-fold to reduce the concentration of denaturant. SDS-PAGE (10% gels) and immunoblot analysis were performed using the mouse anti-V5 primary antibody followed by HRP-conjugated donkey anti-mouse (sc-2314, Santa Cruz Biotechnology).

Stability of CEL-WT and CEL-MUT Proteins in a Proteasome- and MgATP-enriched Reticulocyte Lysate System—We expressed human CEL-WT and CEL-MUT *in vitro* in a coupled transcription/translation system using rabbit reticulocyte (RRL) lysates (Promega) in a total reaction volume of 50 μl containing 40 μl of RRL, 2 μg of *CEL-WT/CEL-MUT* (in pcDNA3.1/HisB vector), 20 mM DTT, and 10 μCi of [^{35}S]Met. Following incubation at 30 °C for 90 min, we stopped the synthesis by an excess of cold Met. The stability of CEL proteins was then assayed in a final volume of 100 μl containing 15 mM Hepes, pH 7.5, 1 mM DTT, 20 μM cold Met, 15 μl of [^{35}S]Met-labeled CEL proteins, 5 mM $MgCl_2$, 0.5 mM ATP, 10 mM phosphocreatine, creatine phosphokinase (0.2 mg/ml), 2 μM ubiquitin, and 50 μl of freshly thawed RRL. Aliquots were removed at various time points (0–3 h), and the reactions were quenched by SDS sample buffer and heated at 56 °C for 15 min prior to SDS-PAGE (10% gel) analysis and autoradiography. The resulting stability graphs represent the average of three independent experimental series for both CEL proteins using different production numbers of the RRL system. The ^{14}C-methylated protein standard contained myosin (220 kDa), phosphorylase *b* (97.4 kDa), BSA (66 kDa), ovalbumin (46 kDa), carbonic anhydrase (30 kDa), and lysozyme (14.3 kDa).

Immunoperoxidase Electron Microscopy—HEK293 cells cultured on plastic culture dishes coated with poly-L-lysine (Sigma) were grown to a confluency of 70–80%, washed with PBS, and fixed with periodate/lysine/paraformaldehyde fixative (21). The pre-embedding immunoperoxidase procedure used for staining of cells with affinity-purified CEL-specific monoclonal As20.1 and goat anti-mouse $F(ab)_2$-fragments coupled HRP (BI3413C, P.A.R.I.S. Anticorps, Compiègne, France) has been described in detail by Brown (22). Thin sections of the immunolabeled cells, embedded in Epon 812 resin (Electron Microscopy Sciences, Hatfield, PA), were stained with lead citrate and examined in a JEOL 1230 (Tokyo, Japan) electron microscope operated at 60 kV.

Collection of Pancreatic and Duodenal Juice—Pancreatic juice was obtained from patients undergoing Whipple's procedure for resection of pancreatic tumor. After transection of the pancreas, the pancreatic duct was cannulated, and a sample of juice was suctioned out and immediately stored on liquid nitrogen. Duodenal juice was obtained by upper endoscopy (Olympus GIF 160, Hamburg, Germany). The procedure was initiated 25 min after stimulation with secretin (Secrelux, Sanochemia Diagnostics (Zug, Switzerland) 1 clinical units/kg, maximum 70 clinical units administered over 1 min), starting with thorough emptying of the ventricle to avoid contamination from gastric contents and continuing with duodenal intubation at 30 min after stimulation. The tip of the endoscope was placed distal to the papilla, and duodenal juice was collected through the suctioning channel as two 5-min aliquots after discharging the juice collected during the 1st min. The aliquots were immediately placed on ice. The samples were then centrifuged at 4400 rpm for 10 min at 4 °C in a table centrifuge and the pellets discarded. We used Complete Mini EDTA-free protease inhibitor (Roche Diagnostics) to protect the samples (1 tablet dissolved in 1.5 ml of water, 0.2 ml of this solution was added per 1 ml of juice). The samples were snap-frozen in liquid nitrogen within 2 h after they had been collected. This procedure was approved by the Institutional Review Board of Western Norway. All subjects had given informed, written consent to the study. The donors of pancreatic and duodenal juice were genotyped as described in Torsvik *et al.* (9).

Computational Analysis—The intrinsically disordered regions in the CEL proteins were predicted by the computer algorithm VSL2P (23), and their propensity to self-associate was predicted by the computer algorithm TANGO (24, 25). We used NetOGlyc 3.1 to explore the *O*-glycosylation sites and Compute p*I*/Mw (26, 27) to determine the p*I* of the two proteins studied.

Statistical Analysis—Analysis of variance was used to analyze differences in gene expression between groups of cells transfected with different constructs. Post hoc pairwise comparisons (Bonferroni method) demonstrated significant effect at a level of 5% using Stata (version 11.0; Stata, College Station, TX).

RESULTS

Physicochemical and Structural Properties of the Wild-type and Mutant CEL Protein—The 79-kDa human CEL-WT protein is characterized by two structural domains, an N-terminal globular catalytic core domain (residues 1–558), including a signal peptide (residues 1–23), and a C-terminal intrinsically highly disordered (random-coiled) extended arm of tandem repeats (TRs, residues 559–745) as shown schematically in Fig. 1*A* (see also supplemental Fig. S1). The 73-kDa CEL-MUT protein has the same core structure, but a c.1686delT mutation introduces a frameshift and causes a truncation of the protein resulting in a 72-residue shorter intrinsically disordered TR domain (residues 559–672). Moreover, *in silico* analyses of the frameshift mutation in the TR region of mutant CEL (Fig. 1*B*) revealed a marked increase in the theoretical p*I* of this domain, from pH 3.3 (WT) to 11.8 (MUT), because of a change in the charged residues from 17 Asp/5 Glu to 19 Arg. There is one *N*-glycosylation site predicted in the core domain (N210), and the total number of putative *O*-glycosylation sites at Thr residues in the TR units are predicted to be 36 (WT) and 11 (MUT) (NetOGlyc 3.1 (28)). However, the actual number and structure of the *N*- and *O*-glycans, when stably expressed in cells, have not been determined. In the presence of numerous *O*-glycans in the TR domain of CEL-WT, it may assume a rigid structure similar to the structurally related mucous glycoproteins (29, 30).

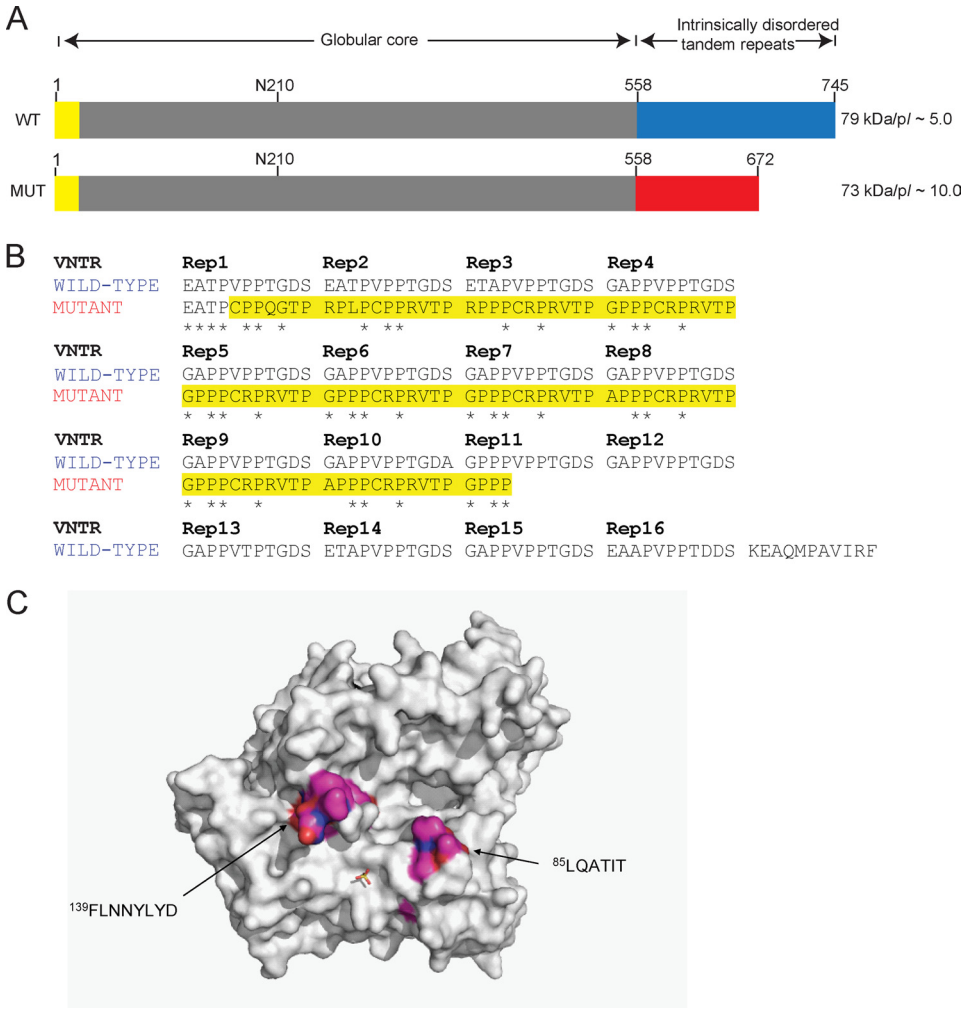

FIGURE 1. **Structure of the human CEL protein variants.** *A*, schematic structure of the CEL-WT and CEL-MUT protein with a globular core domain and an intrinsically disordered C-terminal region consisting of tandem repeats and harboring multiple *O*-glycosylation sites. *B*, alignment of the C-terminal TR regions of CEL-MUT and CEL-WT. Note the change in amino acid composition and the early termination of the mutant protein. *Asterisks* denote unchanged amino acids. *C*, three-dimensional structure of the CEL globular core domain (Protein Data Bank codes 1f6w and 1jmy). Two surface-exposed peptide segments (*red*) with a putative aggregation propensity were predicted by the sequence-based TANGO algorithm.

When the catalytic core domain of CEL is overexpressed in bacteria, it is recovered as inclusion bodies, which are insoluble in 1% (v/v) Triton X-100 and require 8 M urea for their solubilization (31). Moreover, the sequence-based computer algorithm TANGO (24) predicts an aggregation propensity of several peptide segments in the core structure, of which two hydrophobic regions map to the surface in the three-dimensional structure (Protein Data Bank codes 1f6w and 1jmy) of CEL (Fig. 1*C*). Finally, the CEL-WT protein is a client protein for the ER molecular chaperone GRP94, forming an ~1:1 complex that is stabilized by hydrophobic forces (11).

CEL-WT and CEL-MUT Are N- and O-Glycosylated in HEK293 Cells—Because the total number of *O*-glycosylation sites is predicted to be different for CEL-WT and CEL-MUT proteins, we examined this issue more closely in HEK293 cells. Following acetone precipitation of the growth medium, the CEL proteins were subjected to *N*-linked (*N*-glycosidase F) and/or *O*-linked (*O*-glycosidase and neuraminidase) deglycosylation treatment, SDS-PAGE, and immunoblot analysis (for a comparison of antibodies against CEL proteins, see supplemental Fig. S3, *A* and *B*). The analyses revealed that exposure to *N*-glycosidase F resulted in a slight increase in the relative mobility of both CEL proteins (Fig. 2), and incubations with *O*-glycosidase and neuraminidase gave an even larger mobility shift of the WT and the mutant protein. A truncated control variant of the CEL protein (TRUNC; p.Val563X), completely lacking the amino acids encoded by the VNTR region, exhibited only a small change in mobility after treatment with glycosidases. In sum, even though theoretical predictions of *O*-glycosylation sites in the mutated CEL showed loss of several *O*-glycosylation sites, both the wild-type and the mutant protein were found to be *O*-glycosylated when secreted from the cells.

Apparent Rates of Secretion and Cellular Degradation of the CEL-WT and CEL-MUT Proteins Are Similar, and Extracellular CEL-MUT Appears More Stable—In the previous work of Raeder *et al.* (1), it was indicated that the dysfunction caused by CEL-MUT could be due to decreased stability of the mutant protein (based on stable expression in CHO cells). Therefore, we used pulse-chase analysis to examine glycosylation, secretion, and degradation of CEL-WT and CEL-MUT stably expressed in HEK293 cells. After a 5-min pulse, the [^{35}S]Met/Cys-labeled CEL proteins, immunoprecipitated from cell

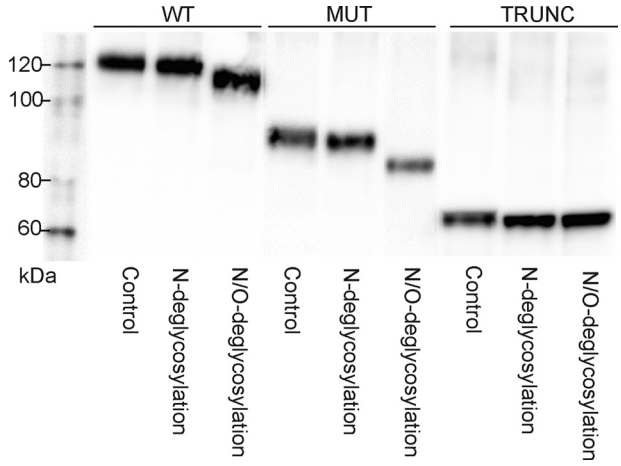

FIGURE 2. ***In vitro N*- and *O*-linked deglycosylation of CEL proteins variants.** Acetone-precipitated proteins from the cell-free growth medium of HEK293 cells, stably expressing CEL-WT and CEL-MUT, were subjected to *N*-linked (*N*-glycosidase F) and/or *O*-linked (*O*-glycosidase and neuraminidase) treatment. A truncated version of the CEL protein (TRUNC), not containing any VNTR-encoded sequence, was included as a control. The Western blots were probed with anti-V5 antibody. Similar mobility shifts were obtained in three independent experiments.

lysates, migrated as double bands on SDS-PAGE. A similar pattern has been reported for the rat CEL protein in an acinar cell line (AR4-2J) and interpreted as post-translational glycosylation at residue Asn-210 (32). During chase, the signal from the lowest band (low molecular mass) decreased, and a higher band, probably representing the *O*-glycosylated forms of the proteins, increased in strength (Fig. 3*A*, CEL-WT (*upper left panel, arrow*) and CEL-MUT (*upper right panel, arrow*)). Both CEL-WT (Fig. 3*A*, *lower left panel*) and CEL-MUT (*lower right panel*) were detectable in the medium after 15 min. The amount of ^{35}S-CEL-WT and ^{35}S-CEL-MUT, both intracellular (*i.e.* soluble in a combined Nonidet P-40/SDS/deoxycholate detergent medium) and extracellular, was determined by phosphorimaging as a function of chase time (Fig. 3*B*). The intensity of the bands of intracellular CEL-MUT peaked at ~15 min chase (Fig. 3*A*, *upper right panel*). At 3 h chase, almost no trace of detergent-soluble cellular CEL-WT and CEL-MUT was observed. At the end point, ~20% (MUT) and ~30% (WT) of the initially labeled proteins were recovered in the growth medium. Replot of data in Fig. 3*B*, with a separate presentation of low molecular mass forms (*arrowheads* in Fig. 3*A*) and the high molecular mass forms (*arrows* in Fig. 3*A*), demonstrated a faster transition from the low to the high molecular mass form of the mutant CEL as compared with the WT. Subsequently, when the recovery of CEL-WT and CEL-MUT proteins was measured after 24 h chase, the secreted mutant protein appeared to be significantly more stable ($p = 0.007$) than the WT protein (Fig. 4, *A* and *B*).

CEL-MUT Protein Generates Higher Oligomeric Forms, and CEL-WT and CEL-MUT Are Both Membrane-associated in the HEK293 Cells—To study a potential aggregation of newly synthesized CEL-WT and CEL-MUT proteins, as they are folded in the HEK293 cells, we performed metabolic labeling before the cells were lysed under nondenaturing conditions, followed by immunoprecipitation. On native-PAGE analyses, some of the dissolved proteins did not enter the running gel, notably the samples with mutant CEL protein, and the protein samples were therefore centrifuged (435,000 × *g* for 1 h at 4 °C), and the recovered supernatants were reexamined by native-PAGE and phosphorimager analysis (Fig. 5*A*). In contrast to the WT CEL protein, the mutant CEL revealed high molecular mass forms both intracellularly and in the growth medium, notably after 45 min of chase. The 435,000 × *g* precipitates were resuspended in sample buffer and subjected to SDS-PAGE and immunoblot analysis using mouse anti-V5 Ab (Fig. 5*B*). In Fig. 5*B*, the *arrowheads* mark the expected monomeric forms of the CEL proteins, and the *arrows* indicate SDS-resistant higher oligomeric forms of CEL-MUT. On SDS-PAGE analysis of the 435,000 × *g* precipitates, only the CEL-MUT revealed higher molecular forms of CEL protein.

Because the CEL-MUT protein revealed a propensity to form high molecular mass forms/aggregates, we next compared the intracellular distribution of the mutant and WT proteins. On subcellular fractionation, both proteins were recovered partly in the pellet (CEL-MUT ≫ CEL-WT) and partly in the supernatant fractions on centrifugation of the post-nuclear supernatant fraction at 3,000 × *g* for 10 min. In cells expressing CEL-MUT, SDS-PAGE and immunoblots of the pellet fraction revealed positive immunoreactivity for α-porin (mitochondrial marker) and Lamp 2 (lysosomal marker) (supplemental Fig. S3*C*). Exposure to Triton X-100 (1% (v/v), 30 min) completely released the WT protein from the pellet fraction, whereas the mutant CEL protein was partly Triton X-100-resistant (Fig. 5*C*). To further analyze the Triton X-100-insoluble fraction, the supernatant and pellet fractions were both treated with 1% (v/v) Triton X-100 for 30 min and centrifuged at 100,000 × *g* for 1 h. The resulting supernatants contained Triton X-100-soluble and the pellets Triton X-100-insoluble, but guanidine chloride-soluble, CEL-MUT protein. The samples that were dissolved in guanidine chloride were diluted 10-fold before SDS-PAGE analysis. Because the diluted samples were prone to precipitate after dilution, they had to be loaded to the gel directly from samples heated to 56 °C. Quantification of the immunoblots revealed that the majority of the CEL-MUT protein was recovered in the Triton X-100-insoluble fraction (Fig. 5, *D* and *E*). Immunoreactive truncated forms (presumably degradation products) were observed in all the fractions analyzed, most prominently in the Triton X-100-soluble CEL proteins; these bands represented 18–24% of the total band intensity. Immunodetection with a ubiquitin-specific antibody did not recognize any bands correlating to an expected size related to CEL-MUT (Fig. 5*D*). Taken together, these results confirm that both the WT and the mutant CEL proteins are membrane-associated and that CEL-MUT has a higher propensity to form higher oligomeric forms and nonubiquitinated aggregates.

Recovery of Intracellular and Extracellular CEL-WT and CEL-MUT Is Increased by Proteasomal and Lysosomal Inhibitors—To investigate the cellular proteolytic systems involved in the quality control of the CEL proteins, we performed pulse-chase experiments after preincubation of HEK293 cells in the presence of inhibitors of the two main pathways. Leupeptin (100 μg/ml), an inhibitor of lysosomal protein degradation, increased the cellular recovery of both the WT (1.6-fold) and the mutant (1.4-fold) CEL proteins (Fig. 6

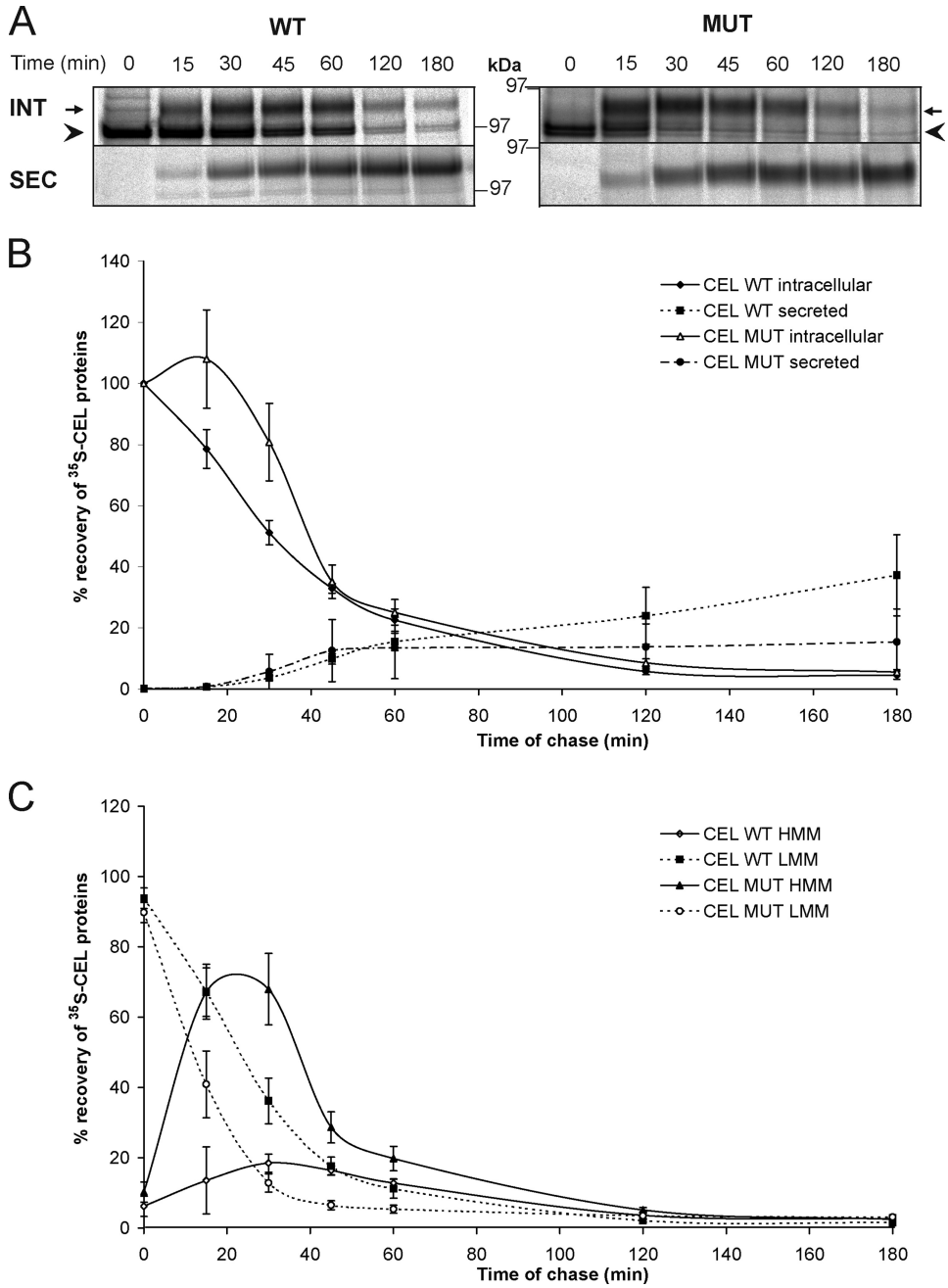

FIGURE 3. **Time course for the secretion of CEL-WT and CEL-MUT by stably transfected HEK293 cells.** *A,* pulse-chase analysis of HEK293 stably expressing CEL-WT (*left panel*) and CEL-MUT (*right panel*). The cells were metabolically labeled with [^{35}S]Met/Cys for 5 min, quickly washed, and chased for indicated time periods. At each time point, cell-free medium was collected; the cells were lysed in a medium containing the detergents Nonidet P-40/SDS/deoxycholate, and lysates (intracellular, *INT*) and medium (secreted, *SEC*) were immunoprecipitated with the monoclonal anti-V5 antibody followed by SDS-PAGE (4–12%). Representative autoradiograms are shown where the *arrowheads* indicate the position of the partly modified CEL proteins, and the *arrows* point to the fully glycosylated CEL proteins. *B,* amount of ^{35}S-CEL-WT and ^{35}S-CEL-MUT, intracellular and extracellular, determined by phosphorimaging and plotted as a function of chase time. Single experiments were performed with triplicate samples at each time point, and the mean of triplicates was normalized by reference to the mean at time 0. Data represent the mean of four independent experiments where *error bars* represent 1 S.D. *C,* replot of data from *B* with separate presentation of detergent-soluble low molecular mass forms (*LMM, arrowheads* in *A*) and high molecular mass forms (*HMM, arrows* in *A*).

and Table 1). The proteasome inhibitor MG132 (10 μM) also increased the cellular recovery of WT and mutant CEL 2.6- and 2.1-fold, respectively. A similar increase was observed for the CEL proteins in the medium with a 2.7- and 3.3-fold increase in the WT and mutant form, respectively. With leupeptin, the effect seen on the secreted protein was similar to the intracellular effect for CEL-WT (*i.e.* a 1.7-fold increase), whereas the recovery of extracellular mutant protein was increased (2.7-fold). In conclusion, both the proteasomal and the lysosomal quality control systems appear to be involved in the clearance of the CEL proteins.

Expression and Degradation of CEL-WT and CEL-MUT Proteins in an in Vitro Reticulocyte Lysate System—A proteasome-dependent degradation of the CEL proteins was further studied in an RRL system (Fig. 7). ^{35}S-CEL proteins, synthesized in the coupled transcription-translation system, revealed high molec-

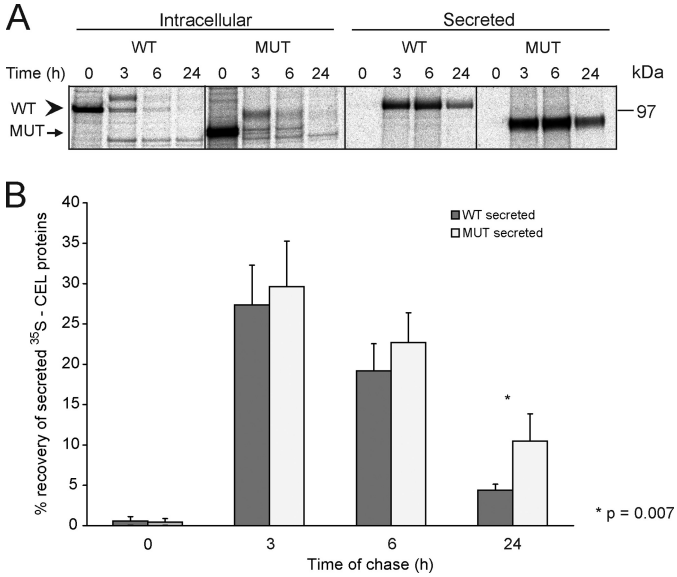

FIGURE 4. **Prolonged time course for the secretion of CEL.** CEL-MUT protein appears to be more stable than the CEL-WT. HEK293 cells were metabolically labeled and chased for the indicated time periods, and the proteins in cell extract and growth medium were immunoprecipitated and analyzed by SDS-PAGE. *A*, representative autoradiograms of cellular (detergent-soluble) and secreted CEL-WT and CEL-MUT. *B*, relative amounts of ^{35}S-CEL-WT and ^{35}S-CEL-MUT determined as a function of chase time. Single experiments were performed in triplicate, and the mean was normalized by reference to the mean at time 0. Data represent the mean of three independent experiments where *error bars* represent 1 S.D.

ular mass bands in addition to the monomeric forms of full-length CEL-WT (Fig. 7*A, 3rd lane*) and CEL-MUT (*4th lane*). Because protein glycosylation does not occur in this cell-free system, we presumed that the high molecular mass forms were the expected ubiquitinated forms (3). When the stability of the monomeric and modified forms was followed over time, both CEL proteins were rapidly degraded (Fig. 7*B*). The degradation of total CEL-MUT was faster than CEL-WT, with only 50% of protein remaining after ~50 min *versus* ~120 min for the WT protein (Fig. 7*C*).

CEL-MUT Appears as Intra- and Extracellular Aggregates—Secreted CEL-MUT protein revealed higher stability than the WT protein (Fig. 4, *A* and *B*) and has a high propensity to self-associate (Fig. 5, *A* and *B*). We therefore performed immunoperoxidase electron microscopy using the CEL-specific monoclonal As20.1 antibody to study the cellular localization of the proteins at the ultrastructural level. In contrast to CEL-WT (Fig. 8*B*), the mutant protein forms extracellular aggregates lining the surface of the plasma membrane (Fig. 8*A*). These aggregates were a typical feature of the CEL-MUT-expressing cells, but they were completely absent from the wild-type cells. Examination of EM sections prepared from CEL-MUT-expressing cells showed the presence of 5.6 ± 2.9 aggregates of varying size but with similar structure at their surface. The aggregates were also found intracellularly, in the lumen of large sized vacuoles limited by a single membrane, possibly representing autophagolysosomes (Fig. 8, *C* and *D*).

CEL Expression Activates the Unfolded Protein Response— The ER is the first compartment of the secretory pathway where proteins fold and are modified by post-translational modifications. Both an elevated synthesis of CEL proteins (stably expressed in the cells) and the expression of a mutant misfolded CEL protein may perturb the ER homeostasis and lead to an accumulation of misfolded proteins triggering the unfolded protein response (UPR). The UPR signals through three branches, under the control of the ER stress transducers IRE1, ATF6, and PERK. IRE1 activation leads to unconventional splicing of *XBP1* mRNA; ATF6 up-regulates the ER chaperone BiP, and activation of the kinase PERK results in phosphorylation of the eukaryotic translation initiation factor eIF2α. To investigate whether the UPR was activated in the stably transfected HEK293 cells, markers for the three branches of the UPR were examined. A truncated version of the CEL protein (TRUNC; p.Val563X) was also included in these experiments to distinguish whether any effects observed would be due to the new C terminus or to the lack of the normal VNTR-encoded sequence.

Real time PCR analysis measuring the levels of spliced *XBP1* mRNA showed no statistically significant difference between cells expressing the two CEL variants and WT-expressing cells, suggesting that the IRE1 branch of the UPR was not activated (Fig. 9*A*). Nor was there any transcriptional activation or increased translation of the ER molecular chaperone BiP (Fig. 9*B*), a key UPR target gene and master regulator of UPR (33). However, an induction of the PERK branch of the UPR was detected in the cells expressing the mutant CEL protein, as demonstrated by significantly increased level of phosphorylated eIF2α and up-regulation of the downstream transcription factor gene *CHOP* (Fig. 9*C*). This transcription factor has been shown to be pro-apoptotic in some cell types, but the increase in *CHOP* mRNA in the CEL protein-expressing cell lines did not result in any significant growth inhibition or cell death (see supplemental Figs. S4 and S5).

Detection of CEL Proteins in Pancreatic and Duodenal Juice of Normal Controls and CEL Mutation Carriers—To determine whether mutant *CEL* products are secreted from acinar cells *in vivo*, the proteins in pancreatic and duodenal juice from normal and *CEL* mutation carriers were examined by SDS-PAGE and immunoblotting (see supplemental material) using CEL-specific antibodies (Fig. 10). In pancreatic juice from a *CEL* mutation carriers, the antibody detected close to equal amounts of normal and mutant variants of the protein (Fig. 10*A*, *4th lane*), indicating that the CEL-WT and CEL-MUT proteins both are secreted at high levels. By contrast, in duodenal juice from two other *CEL* mutation carriers, the antibody detected far less mutant protein than normal protein (Fig. 10*B*, *3rd* and *4th lanes*), suggesting a relative loss of mutant protein in the transport from pancreas to duodenum. However, in duodenal juice from a control, both the allelic variants of the protein were present (Fig. 10*C*). Interestingly, when examining the urine from normal and *CEL* mutation carriers in a related study, Raeder *et al.* (1) were able to detect the normal but not the mutant protein. Taken together, these observations suggest that the mutant CEL protein is secreted from the acinar cells but is partly degraded and aggregated on its way from the pancreatic duct.

DISCUSSION

The CEL protein is a carboxyl ester lipase expressed in the acinar cells and secreted as a component of pancreatic juice.

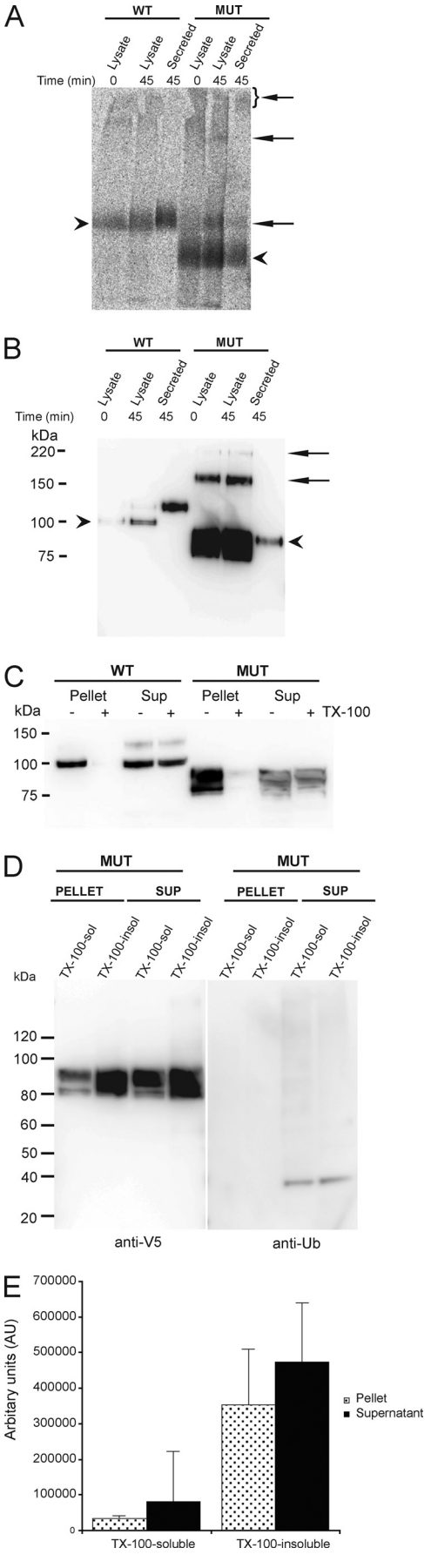

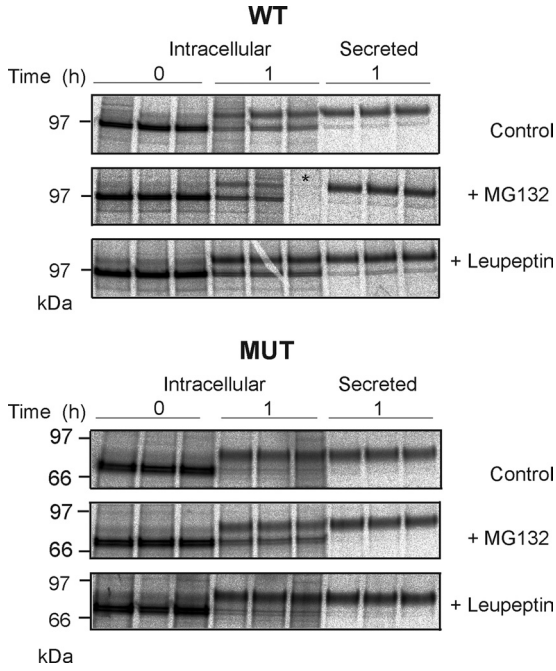

FIGURE 6. **Cellular stability of CEL-WT and CEL-MUT proteins is increased in cells exposed to proteasomal and lysosomal inhibitors.** Representative autoradiograms of cellular and secreted CEL-WT and CEL-MUT proteins are shown. The effect of protease inhibitors on the cellular stability of CEL-WT and CEL-MUT was determined by incubating the HEK293 cells in the presence and absence of 100 μg/ml leupeptin (lysosome inhibitor) or 10 μM MG132 (proteasome inhibitor) for 3 h prior to [^{35}S]Met/Cys labeling. Metabolically labeled cells were chased for 1 h, and CEL proteins in extracts and medium were immunoprecipitated and analyzed by SDS-PAGE. An *asterisk* denotes an empty lane in WT panel 2 (+*MG132*).

The biosynthesis, post-translational modifications, and secretion of the rat CEL enzyme have been studied in detail in the AR4-2J acinar cell line (reviewed in Ref. 3), and these data served as a main reference in this study on the human enzyme. When we stably expressed the WT and MUT human CEL proteins in HEK293 cells, they were both, as expected, *N*- and *O*-glycosylated (Fig. 2). In addition, both were secreted constitutively, although at somewhat different rates. Thus, in the first

FIGURE 5. **CEL-MUT protein forms higher oligomeric forms that are SDS-resistant and Triton X-100-insoluble.** *A,* metabolically labeling of HEK293 cells, stably expressing CEL-WT (*left panel*) and CEL-MUT (*right panel*). Subsequently, the cells were lysed, and the CEL proteins His tag affinity-purified as described under "Experimental Procedures." The eluted CEL proteins were centrifuged (435,000 × *g* for 1 h at 4 °C); the supernatants were analyzed by native-PAGE, and the gels were dried and detected using a phosphorimager. *B,* SDS-PAGE of the pelleted protein. The pellets were resuspended in 2× sample buffer and subjected to SDS-PAGE followed by immunoblot analysis; CEL proteins were detected by monoclonal anti-V5. The *arrowheads* in *A* and *B* indicate the expected monomeric forms of the CEL proteins, and the *arrows* indicate higher oligomeric forms of CEL-MUT (SDS-resistant in *B*). *C,* subcellular fractionation of CEL-WT and CEL-MUT. After centrifugation of lysed cells at 3000 × *g* for 10 min, both proteins were recovered partly in the pellet fraction (CEL-MUT ≫ CEL-WT) and partly in the supernatant (*Sup*). Triton X-100 (*TX-100*) (30-min exposure) completely released the WT protein from the pellet fraction (*i.e.* no pellets when rerun at 3,000 × *g* for 10 min), whereas CEL-MUT was partly Triton X-100-resistant. *D* and *E,* analysis of Triton X-100-soluble and -insoluble CEL-MUT. The majority of the CEL-MUT protein is Triton X-100-insoluble and not ubiquitinated. Alternatively, 3,000 × *g* cell fractions (supernatant and pellet) were treated with 1% (v/v) Triton X-100 for 30 min and centrifuged at 100,000 × *g* for 1 h. The supernatants contained Triton X-100-soluble and the pellets Triton X-100-insoluble, but guanidine chloride-soluble, CEL proteins. The fractions were subjected to SDS-PAGE as described under "Experimental Procedures," and the CEL proteins were quantified by immunodetection ($n = 9$).

45 min of the pulse-chase experiments, the MUT protein was apparently *O*-glycosylated faster than the WT form (Fig. 3*C*). The higher initial rate of glycosylation of the mutant protein may be related to its fewer potential *O*-glycosylation sites and/or to its different primary structure and physicochemical properties of the TR domain, which may favor the accessibility to various glycoprotein glucosyltransferases. However, in a 3-h time frame, the overall recovery of soluble CEL in the medium appeared highest in cells expressing the WT protein. Thus, ~30% (WT) and ~20% (MUT) of the initially labeled detergent-soluble CEL protein was recovered as soluble protein after 3 h (Fig. 3*B*), and the intracellularly retained proteins revealed a different subcellular distribution and solubility. Whereas the WT protein gave an approximately equal recovery in the pellet and the supernatant fraction on centrifugation of the post-nuclear supernatant fraction at 3,000 × *g* for 10 min, the majority of the mutant protein was recovered in the pellet fraction (Fig. 5*C*) enriched in mitochondria, lysosomes, and lysosome-derived organelles. Moreover, although Triton X-100 completely released the WT protein from the pellet fraction, the mutant CEL protein was partly Triton X-100-resistant but soluble by chemical denaturation in guanidine chloride (Fig. 5, *D* and *E*).

In addition to the expected *N*- and *O*-glycosylation and transport of both CEL proteins along an apparently regular route of the secretory pathway, our pulse-chase analysis (Figs. 3 and 4) and subcellular fractionations (Fig. 5) suggest that both proteins are retrotranslocated from the ER to the cytoplasm. This pathway, representing transport of overexpressed and presumably terminally misfolded forms of CEL proteins, is partly linked to the ubiquitin-proteasome system as observed previously for rat CEL in an AR4-2J pancreatic cell line (34). Thus, when the proteasomal proteolytic activity is blocked, the recovery of detergent-soluble cellular CEL proteins increased (Fig. 6). In addition to this quality control by the ER-associated degradation machinery, both proteins accumulate in a large granule pellet fraction, sedimentable from a post-nuclear supernatant fraction at a low centrifugal effect (3,000 × *g* for 10 min) (Fig. 5*C*). Furthermore, when the lysosomal proteolytic activity was inhibited by leupeptin, the recovery of detergent-soluble cellular CEL proteins increased (Fig. 6), indicating a delayed clearance of both proteins by autophagy. In the case of the CEL-MUT protein, aggregates were seen intracellularly in the lumen of large sized vacuoles throughout the cytoplasm. Immunoperoxidase electron microscopy identified some of

TABLE 1

Quantification of effect of proteasomal and lysosomal inhibitors on stability of CEL proteins

The amounts of ^{35}S-CEL-WT and ^{35}S-CEL-MUT proteins were determined using a phosphorimager. Single experiments were normalized by reference to the mean at time 0 (100%). The table represents fold increase in ^{35}S-CEL protein level at 1 h of chase relative to the untreated control. The data represent the mean of triplicate determinants ± S.D. from a single experiment. Three independent experiments obtained similar results.

	MG132		Leupeptin	
	Intracellular	Secreted	Intracellular	Secreted
WT	2.6 ± 0.32	2.7 ± 0.21	1.6 ± 0.09	1.7 ± 0.27
MUT	2.1 ± 0.15	3.3 ± 0.47	1.4 ± 0.06	2.7 ± 0.53

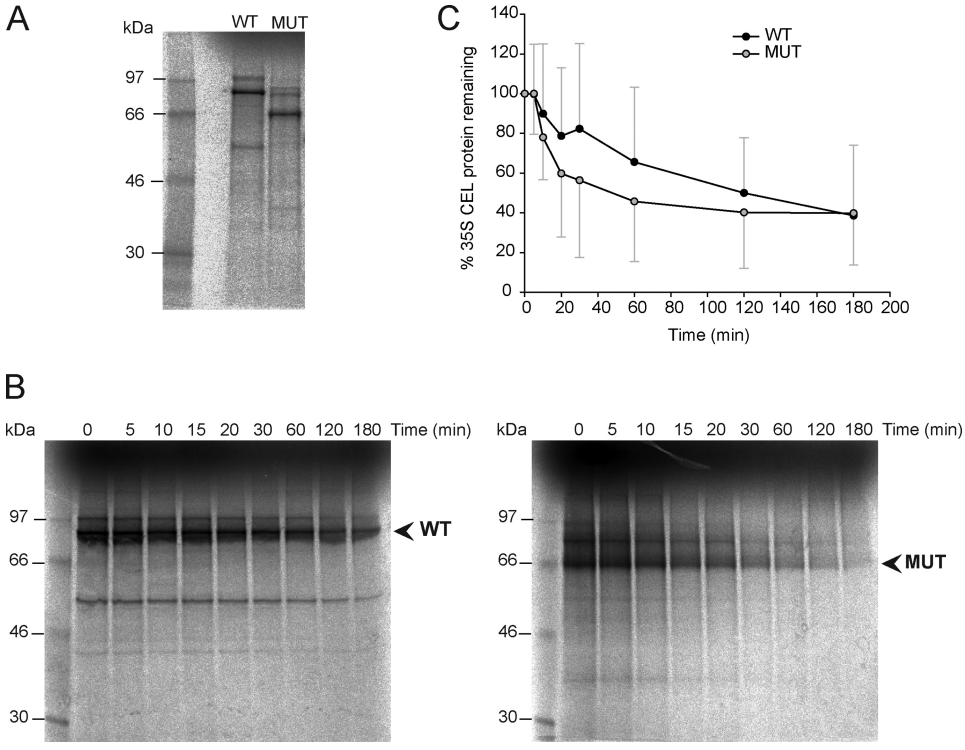

FIGURE 7. **Expression and stability of CEL-WT and CEL-MUT proteins in an *in vitro* RRL system.** CEL-WT and CEL-MUT were expressed in a reconstituted RRL system as described under "Experimental Procedures." *A,* autoradiogram of total [^{35}S]Met-labeled translation products (reaction time 90 min at 30 °C) analyzed by SDS-PAGE (10% gel) with CEL-WT (*3rd lane*) and CEL-MUT (*4th lane*). *B,* stability of CEL-WT and CEL-MUT followed over time in a proteasome- and MgATP-enriched RRL system. Protein samples were analyzed by SDS-PAGE (10% gel) and phosphorimager analysis. Representative gels are shown for CEL-WT and CEL-MUT. The *arrowheads* indicate the translation products whereas the higher molecular mass bands represent post-translationally modified (ubiquitinated) forms of CEL proteins. *C,* time course for the decay of [^{35}S]Met-labeled CEL-WT (■) and CEL-MUT (○) proteins. The *graphs* represent the average of three independent experiments using different production numbers of the RRL; the *bars* represent 1 S.D.

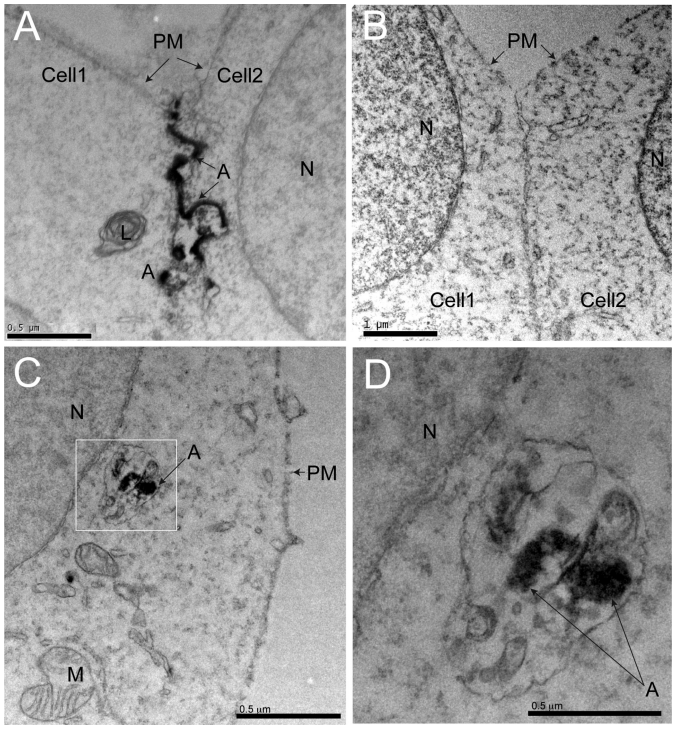

FIGURE 8. **CEL-MUT forms extra- and intracellular aggregates in HEK293 cells.** HEK293 cells stably transfected with CEL-MUT and CEL-WT were processed for immunoperoxidase electron microscopy as described under "Experimental Procedures." *A*, extracellular CEL-MUT protein aggregate lining the surface of the plasma membrane. *B*, CEL-WT-expressing cells are devoid of such structures. *C* and *D*, intracellular CEL-MUT aggregates in the lumen of a large sized vacuole limited by a single membrane (highlighted in *D*) possibly representing an autophagolysosome. *A*, aggregated CEL-MUT protein; *L*, lysosome; *N*, nucleus; *PM*, plasma membrane; *M*, mitochondria, *Bars*, 0.5 μm (*A*, *C*, and *D*) and 1 μm (*B*).

these structures as single membrane-enclosed protein aggregates, characteristic of autophagolysosomes (Fig. 8, *C* and *D*). This interpretation is further supported by confocal microscopy showing that the CEL-MUT-containing vacuoles are surrounded by Lamp-1-positive membranes.[3] The pathway(s) to autophagy has, however, not yet been defined. For the mutant protein, our studies indicate that the subpopulation of guanidine chloride-soluble aggregates was devoid of ubiquitination (Fig. 5*D*) excluding a pathway involving aggresome formation (35) and selected autophagy (reviewed in Ref. 36). Alternatively, a subpopulation of CEL-MUT may be sequestered to a subcompartment of the ER and ultimately cleared by autophagy, as shown for several secretory proteins (reviewed in Ref. 37). Additionally, immunoperoxidase-positive CEL protein aggregates were found to line the cell membranes (Fig. 8*A*). Because this microscopic pattern was observed only in cells expressing the mutant protein, it is likely to be related to its higher propensity to self-associate and possibly also to form complexes with other cellular proteins and cell membranes.

Native-PAGE analysis of the ^{35}S-labeled CEL-MUT protein from cell extracts with detergents revealed radioactive bands corresponding to higher order oligomeric forms in addition to the protomers (Fig. 5*A*), and on SDS-PAGE an apparently SDS-stable dimer (~150 kDa) is observed (Fig. 5*B*). The formation of this dimeric species, and the larger oligomeric forms and aggregates, may tentatively be related to the putative amyloidogenic sequence motifs exposed on the surface of the globular core domain (Fig. 1*C*), previously shown to be prone to aggregation. Thus, when overexpressed in bacteria as a nonglycosylated truncated form, it is recovered in inclusion bodies (31). However, in extracts of cells expressing the CEL-WT protein such a SDS-stable dimer is not observed, lending support to the idea of a protective effect by its highly negatively charged and glycosylated C-terminal TR domain, which is not the case for the mutant CEL protein. Whereas the core structure has a theoretical p*I* of 9.4, and a net positive charge at neutral pH, the two TR domains have theoretical p*I* values of 3.3 (WT) and 11.8 (mutant); at physiological pH values, the WT TR has a net negative change of −22 and the mutant TR a net positive charge of +19. Both TR domains are highly hydrophilic and should be water-soluble, and any additional *O*-linked glycan chains may further contribute to their overall hydrophilicity and solubility. It is therefore likely that the different physicochemical properties (sequence, p*I*, and number of potential glycosylation sites) of the two intrinsically disordered TR domains contribute to different short and long range interactions with the globular core domain and with other macromolecules, including membranes.

Cell degeneration in amyloid diseases may be mediated by a toxic mechanism involving the insertion of aggregated species with the plasma membrane of affected cells (38). One example is pancreatic beta cell failure related to the formation of islet amyloid deposit of the 37-residue natively unfolded human islet amyloid polypeptide (IAPP). Negatively charged lipid membranes and lipid rafts favor the binding of IAPP and also promote its aggregation (39). A positively charged N terminus is considered responsible for the partial insertion of IAPP into negatively charged lipid membranes, a process mainly driven by electrostatic interactions (39). Similarly, the highly positively charged TR domain of CEL-MUT would favor its interaction with membranes (phospholipid headgroups) as actually observed as aggregates at the plasma membrane of HEK293 cells in this study (Fig. 8*A*). Moreover, on overexpression of CEL-MUT in HEK293 cells (this study) and expression in pancreatic acinar cells *in vivo*, macromolecular crowding is expected to promote aggregation of the mutant protein, both in the cytosol and extracellularly at high protein concentrations. Thus, crowding promotes self-association of other natively unfolded proteins (40). Finally, on co-expression of CEL-WT and CEL-MUT proteins, as is the case in heterozygote patients, the mutant protein may induce a co-aggregation of mutant and WT protein (forming hetero-oligomers) by an electrostatic interaction between their TR domains of opposite charge and thus contribute a negative complementation effect. However, preliminary analyses of pancreatic and duodenal juice from heterozygous patients with *CEL*-MODY (Fig. 10) do not support such an effect.

The overexpression of the CEL-MUT protein in HEK293 cells results in an activation of the PERK signaling pathway of the UPR. The UPR is an adaptive response to unfolded or misfolded protein accumulation in the ER, but when prolonged or

[3] J. Torsvik, B. B. Johansson, M. Marie, S. Johansson, H. Ræder, J. Saraste, P. R. Njølstad, and A. Molven, manuscript in preparation.

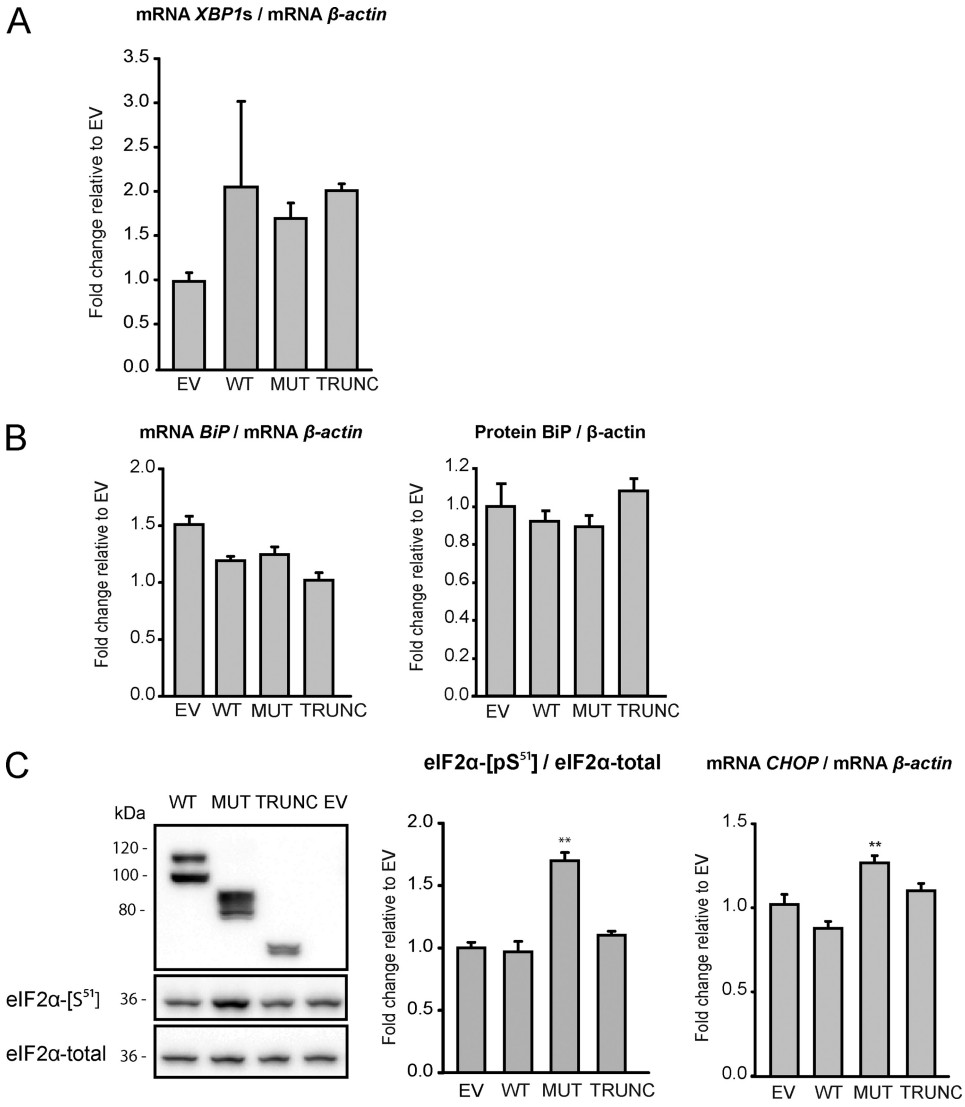

FIGURE 9. **UPR in HEK293 cells expressing different CEL proteins.** Detergent-soluble proteins in lysates of cells expressing CEL-WT, CEL-MUT, and EV were analyzed by immunoblotting using specific antibodies (see under "Experimental Procedures"). A truncated version of the CEL protein (TRUNC, p.Val563X), was included as a control. mRNA levels were measured by quantitative real time PCR, normalized to the housekeeping gene *β-actin,* and reported as fold induction compared with the level of control cells (*EV*). *A, XBP1* mRNA splicing in cell lines stably expressing CEL proteins. *B,* mRNA and protein expression of the ER molecular chaperone BiP (GRP78). *C,* analysis of the PERK branch. Phosphorylation of the transcriptional initiation factor eIF2α (*eIF2α-[pS^{51}]*) and total eIF2α protein in representative blots and densitometric quantification, and mRNA expression of the downstream transcription factor *CHOP*. Results are given as mean ± S.E. of three to five independent experiments. **, $p < 0.01$; *versus* EV.

severe, the response may be deleterious to the cell. The observed activation of PERK in CEL-MUT-expressing cells (Fig. 9*C*) seems to be beneficial rather than detrimental in our cell culture model. Our overall data support a beneficial effect because of the following: (i) the activation of the transducer was mild (Fig. 9*C*); (ii) the misfolded CEL-MUT protein in the ER lumen is largely "retrotranslocated" to the cytoplasm where it is accumulated in cell organelles (Fig. 5) recovered in a fraction containing lysosomes and autophagolysosomes and partly degraded by the ER-associated degradation system, considered to be regulated by the UPR (41), and (iii) the activation of the PERK/eIF2α phosphorylation pathway may represent a cellular defense system by activation of autophagy as shown for the degradation of polyglutamine (polyQ72) aggregates in C2C5 cells (42). Additionally, an interaction of CEL-MUT with essential cellular proteins, which could become inactivated, depleted, or erroneously activated, should be considered.

Ongoing studies using pancreatic tissue from a CEL-MODY patient indicate that CEL-MUT somehow causes inflammatory changes in pancreatic tissue suggesting a cytotoxic link between CEL-MUT and cellular proteins.[4]

The question is now to what extent the physicochemical properties and cellular behavior of the CEL-MUT protein, in particular its differences from the WT variant, relate to the acinar cells and the findings in patients. *CEL*-MODY is a syndrome of pancreatic exocrine dysfunction and diabetes because of mutations in *CEL* (1). Pancreatic lipomatosis and exocrine dysfunction is found from childhood in this syndrome preceding the development of diabetes, which usually appears at 30–40 years of age (43). *CEL*-MODY is likely to be initiated in the acinar tissue, and a loss-of-function of the mutant protein

[4] H. Raeder, P. R. Njølstad, A. Molven, and R. N. Kulkarni, unpublished data.

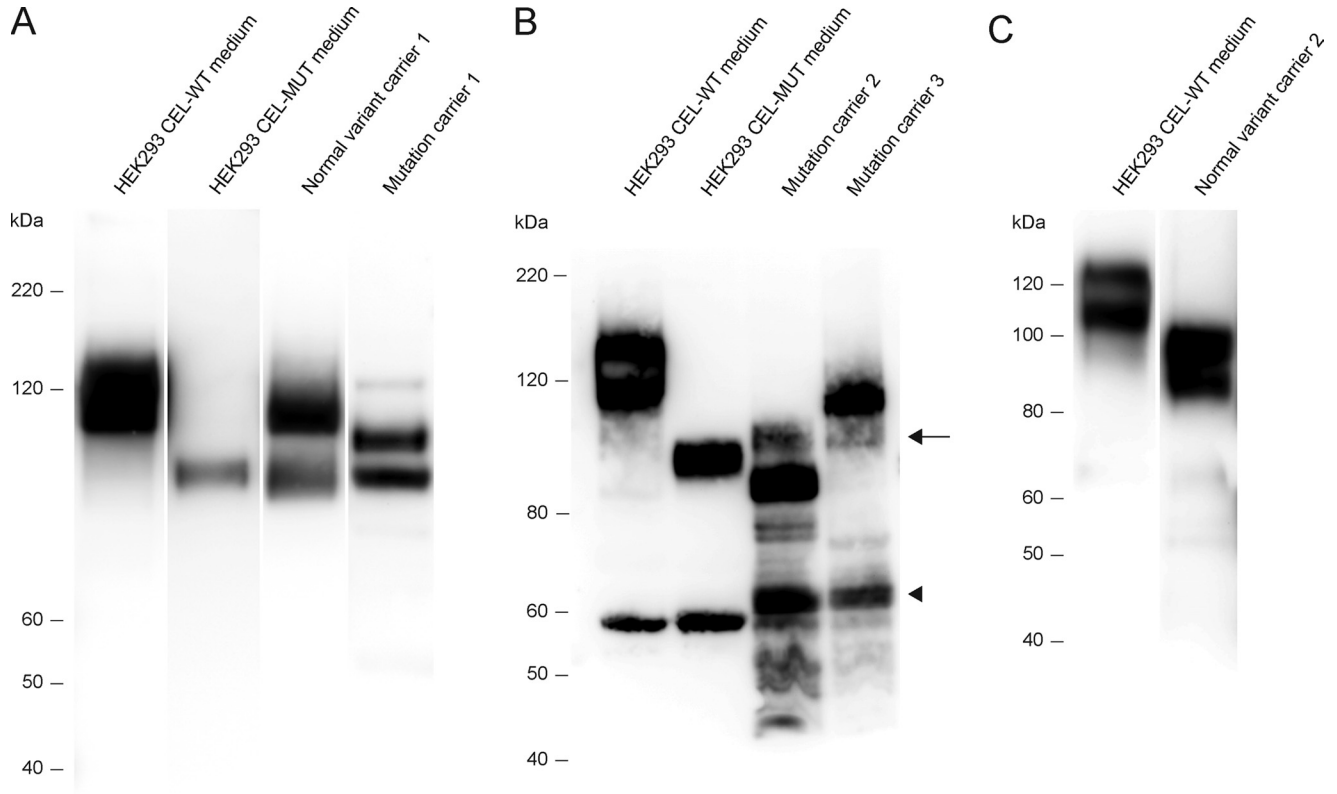

FIGURE 10. **Detection of CEL proteins in pancreatic and duodenal juice of normal controls and *CEL* mutation carriers.** *A,* immunoblot of CEL proteins in pancreatic juice obtained from subjects carrying normal or normal/mutant *CEL*, respectively, using the pAbL64 antibody. *1st lane*, HEK293 CEL-WT medium; *2nd lane*, HEK293 CEL-MUT medium; *3rd lane*, normal *CEL* carrier 1: two major bands corresponding to the gene products of two alleles carrying 16 (*upper band*) and 13 (*lower band*) VNTR repeats, respectively; *4th lane*, *CEL* mutation carrier 1: two major bands corresponding to the gene products of one normal allele carrying 16 VNTR repeats (*upper band*) and a mutant 14-repeat allele carrying the mutation (*lower band*). *B* and *C,* immunoblots of CEL proteins in duodenal juice obtained from subjects carrying mutant (*B*) and normal (*C*) variants of the *CEL* gene, respectively, using the Ulferts antibody. *B, 1st lane*, HEK293 CEL-WT medium; *2nd lane*, HEK293 CEL-MUT medium; *3rd* and *4th lanes*, *CEL* mutation carriers 2 and 3: two major bands corresponding to the gene products of one normal allele carrying 13* (*3rd lane, lower band*) and 16 (*4th lane, upper band*) VNTR repeats, respectively, and a mutant 14-repeat allele carrying the mutation (*upper band, 3rd lane*, *lower band, 4th lane*, indicated by *arrow*). The low molecular mass bands indicated by the *arrowhead* represent degradation products of the CEL proteins. It should be noted that differences in salt concentration and differences in glycosylation pattern between individuals lead to a slight difference in migration pattern on the gel. Also the sample of pancreatic juice from the mutation carrier was mucous. *C, 1st lane*, HEK293 CEL-WT medium; *2nd lane*, normal *CEL* carrier 2: two major bands corresponding to the gene products of two alleles carrying 16 (*upper band*) and 15 (*lower band*) VNTR repeats, respectively. *, this normal variant harbors an insertion and gives a shortened protein, migrating as ~9 repeats (1).

was initially suggested as a possible mechanism of the disorder (1). However, CEL knock-out mice did not develop exocrine dysfunction or diabetes, suggesting a more complex mechanism of disease development (19). Biochemical and morphological data on the CEL-MUT protein are expressed in HEK293 cells, indicating that the disease pathogenesis may be a sustained and at a certain stage an uncontrolled cellular stimulus related to soluble oligomeric conformations and/or insoluble aggregates of the protein. These forms of the protein can appear intracellular or extracellular, and the syndrome may thus be considered a protein misfolding disease or proteopathy. We suggest that the self-association of the protein from monomers via soluble oligomeric intermediates (Fig. 5) into larger insoluble aggregates (Fig. 8) confers a late onset cytotoxic effect of the mutant protein. When extrapolated to the pancreatic tissue, disease may arise in a way analogous to that observed in pancreatic beta cell failure related to the formation of islet amyloid deposit of IAPP (39), Alzheimer disease (44), and Parkinson disease (45). These amyloid disorders are also associated with an aggregation of intrinsically disordered proteins (45, 46) and a late onset of the clinical manifestations, thus possibly acting as a model for development of exocrine dysfunction and diabetes in *CEL*-MODY patients. Interestingly, protein misfolding is relevant also for another MODY form, in which diabetes may be due to misfolded insulin molecules (47, 48).

Immunoblots of the soluble CEL proteins reveal possible degradation products of the CEL-WT and the CEL-MUT proteins, with the size of the core domain protein (~60 kDa), and are also observed together with a smear of additional putative degradation products of CEL in the duodenal juice (Fig. 10*B*). A question is how the mutant protein is lost on its way from the pancreatic duct, where it is detected in amounts comparable with the normal protein, to the duodenum, where it is markedly reduced, and further to the urine, where it is undetectable. One possible explanation can be an increased degradation of the soluble mutant protein. An alternative cause can be that the propensity to aggregate increases outside the pancreas, both due to a lack of stabilizing binding partners and/or interaction with other molecules and membranes, which further can lead to reduced reuptake of the protein in the duodenum. However, the molecular species, assembly, and conformation of the CEL-MUT protein that represents the putative cytotoxic potential

triggering of the disease pathogenesis of the *CEL*-MODY syndrome, the initial stages of the disease, and the time frame in the disease progression remain to be established.

Acknowledgments—Confocal imaging was performed at the Molecular Imaging Center, University of Bergen (FUGE platform, Research Council of Norway). We thank Monika Ringdal, Liv Aasmul, and Gilbert Vandenbroeck for expert technical assistance. The polyclonal L64d antibody detecting CEL was a generous gift from Dominique Lombardo (INSERM U-559, Marseille, France).

REFERENCES

1. Raeder, H., Johansson, S., Holm, P. I., Haldorsen, I. S., Mas, E., Sbarra, V., Nermoen, I., Eide, S. A., Grevle, L., Bjørkhaug, L., Sagen, J. V., Aksnes, L., Søvik, O., Lombardo, D., Molven, A., and Njølstad, P. R. (2006) *Nat. Genet.* **38,** 54–62
2. Roudani, S., Miralles, F., Margotat, A., Escribano, M. J., and Lombardo, D. (1995) *Biochim. Biophys. Acta* **1264,** 141–150
3. Lombardo, D. (2001) *Biochim. Biophys. Acta* **1533,** 1–28
4. Bläckberg, L., Lombardo, D., Hernell, O., Guy, O., and Olivecrona, T. (1981) *FEBS Lett.* **136,** 284–288
5. Nilsson, J., Bläckberg, L., Carlsson, P., Enerbäck, S., Hernell, O., and Bjursell, G. (1990) *Eur. J. Biochem.* **192,** 543–550
6. Lombardo, D., and Guy, O. (1980) *Biochim. Biophys. Acta* **611,** 147–155
7. Higuchi, S., Nakamura, Y., and Saito, S. (2002) *J. Hum. Genet.* **47,** 213–215
8. Lindquist, S., Bläckberg, L., and Hernell, O. (2002) *Eur. J. Biochem.* **269,** 759–767
9. Torsvik, J., Johansson, S., Johansen, A., Ek, J., Minton, J., Raeder, H., Ellard, S., Hattersley, A., Pedersen, O., Hansen, T., Molven, A., and Njølstad, P. R. (2010) *Hum. Genet.* **127,** 55–64
10. Bruneau, N., and Lombardo, D. (1995) *J. Biol. Chem.* **270,** 13524–13533
11. Bruneau, N., Lombardo, D., and Bendayan, M. (1998) *J. Cell Sci.* **111,** 2665–2679
12. Wang, C. S., Dashti, A., Jackson, K. W., Yeh, J. C., Cummings, R. D., and Tang, J. (1995) *Biochemistry* **34,** 10639–10644
13. Reue, K., Zambaux, J., Wong, H., Lee, G., Leete, T. H., Ronk, M., Shively, J. E., Sternby, B., Borgström, B., and Ameis, D. (1991) *J. Lipid Res.* **32,** 267–276
14. Rogers, S., Wells, R., and Rechsteiner, M. (1986) *Science* **234,** 364–368
15. Pasqualini, E., Caillol, N., Valette, A., Lloubes, R., Verine, A., and Lombardo, D. (2000) *Biochem. J.* **345,** 121–128
16. Verine, A., Le Petit-Thevenin, J., Panicot-Dubois, L., Valette, A., and Lombardo, D. (2001) *J. Biol. Chem.* **276,** 12356–12361
17. Lombardo, D., Guy, O., and Figarella, C. (1978) *Biochim. Biophys. Acta* **527,** 142–149
18. Vesterhus, M., Raeder, H., Johansson, S., Molven, A., and Njølstad, P. R. (2008) *Diabetes Care* **31,** 306–310
19. Vesterhus, M., Raeder, H., Kurpad, A. J., Kawamori, D., Molven, A., Kulkarni, R. N., Kahn, C. R., and Njølstad, P. R. (2010) *Pancreatology* **10,** 467–476
20. Sannerud, R., Marie, M., Hansen, B. B., and Saraste, J. (2008) *Methods Mol. Biol.* **457,** 253–265
21. McLean, I. W., and Nakane, P. K. (1974) *J. Histochem. Cytochem.* **22,** 1077–1083
22. Brown, W. J. (ed) (1999) *Immunoperoxidase Methods for Localization of Antigens in Cultured Cells and Tissues*, Vol. 4.6.1–4.6.17, John Wiley & Sons, Inc., New York
23. Obradovic, Z., Peng, K., Vucetic, S., Radivojac, P., and Dunker, A. K. (2005) *Proteins* **61,** Suppl. 7, 176–182
24. Fernandez-Escamilla, A. M., Rousseau, F., Schymkowitz, J., and Serrano, L. (2004) *Nat. Biotechnol.* **22,** 1302–1306
25. Linding, R., Schymkowitz, J., Rousseau, F., Diella, F., and Serrano, L. (2004) *J. Mol. Biol.* **342,** 345–353
26. Bjellqvist, B., Basse, B., Olsen, E., and Celis, J. E. (1994) *Electrophoresis* **15,** 529–539
27. Bjellqvist, B., Hughes, G. J., Pasquali, C., Paquet, N., Ravier, F., Sanchez, J. C., Frutiger, S., and Hochstrasser, D. (1993) *Electrophoresis* **14,** 1023–1031
28. Julenius, K., Mølgaard, A., Gupta, R., and Brunak, S. (2005) *Glycobiology* **15,** 153–164
29. Rose, M. C., Voter, W. A., Brown, C. F., and Kaufman, B. (1984) *Biochem. J.* **222,** 371–377
30. Marianne, T., Perini, J. M., Lafitte, J. J., Houdret, N., Pruvot, F. R., Lamblin, G., Slayter, H. S., and Roussel, P. (1987) *Biochem. J.* **248,** 189–195
31. Terzyan, S., Wang, C. S., Downs, D., Hunter, B., and Zhang, X. C. (2000) *Protein Sci.* **9,** 1783–1790
32. Abouakil, N., Mas, E., Bruneau, N., Benajiba, A., and Lombardo, D. (1993) *J. Biol. Chem.* **268,** 25755–25763
33. Bertolotti, A., Zhang, Y., Hendershot, L. M., Harding, H. P., and Ron, D. (2000) *Nat. Cell Biol.* **2,** 326–332
34. Le Petit-Thevenin, J., Verine, A., Nganga, A., Nobili, O., Lombardo, D., and Bruneau, N. (2001) *Biochim. Biophys. Acta* **1530,** 184–198
35. Chin, L. S., Olzmann, J. A., and Li, L. (2010) *Biochem. Soc. Trans.* **38,** 144–149
36. Kirkin, V., McEwan, D. G., Novak, I., and Dikic, I. (2009) *Mol. Cell* **34,** 259–269
37. Buchberger, A., Bukau, B., and Sommer, T. (2010) *Mol. Cell* **40,** 238–252
38. Kagan, B. L., Azimov, R., and Azimova, R. (2004) *J. Membr. Biol.* **202,** 1–10
39. Weise, K., Radovan, D., Gohlke, A., Opitz, N., and Winter, R. (2010) *ChemBioChem* **11,** 1280–1290
40. Munishkina, L. A., Ahmad, A., Fink, A. L., and Uversky, V. N. (2008) *Biochemistry* **47,** 8993–9006
41. Werner, E. D., Brodsky, J. L., and McCracken, A. A. (1996) *Proc. Natl. Acad. Sci. U.S.A.* **93,** 13797–13801
42. Kouroku, Y., Fujita, E., Tanida, I., Ueno, T., Isoai, A., Kumagai, H., Ogawa, S., Kaufman, R. J., Kominami, E., and Momoi, T. (2007) *Cell Death Differ.* **14,** 230–239
43. Raeder, H., Haldorsen, I. S., Ersland, L., Grüner, R., Taxt, T., Søvik, O., Molven, A., and Njølstad, P. R. (2007) *Diabetes* **56,** 444–449
44. Broersen, K., Rousseau, F., and Schymkowitz, J. (2010) *Alzheimers Res. Ther.* **2,** 12
45. Uversky, V. N., and Eliezer, D. (2009) *Curr. Protein Pept. Sci.* **10,** 483–499
46. Uversky, V. N. (2009) *Front. Biosci.* **14,** 5188–5238
47. Støy, J., Edghill, E. L., Flanagan, S. E., Ye, H., Paz, V. P., Pluzhnikov, A., Below, J. E., Hayes, M. G., Cox, N. J., Lipkind, G. M., Lipton, R. B., Greeley, S. A., Patch, A. M., Ellard, S., Steiner, D. F., Hattersley, A. T., Philipson, L. H., and Bell, G. I. (2007) *Proc. Natl. Acad. Sci. U.S.A.* **104,** 15040–15044
48. Molven, A., Ringdal, M., Nordbø, A. M., Raeder, H., Støy, J., Lipkind, G. M., Steiner, D. F., Philipson, L. H., Bergmann, I., Aarskog, D., Undlien, D. E., Joner, G., Søvik, O., Bell, G. I., and Njølstad, P. R. (2008) *Diabetes* **57,** 1131–1135